J. Min. Metall. Sect. B-Metall. 54 (3) B (2018) 401 - 409

Journal of Mining and Metallurgy, Section B: Metallurgy

EFFECT OF ACCUMULATIVE ROLL BONDING PROCESS ON TEXTURAL EVOLUTION AND ITS COMPARISON WITH NORMAL ROLLED AA7005 ALUMINUM ALLOY

H. Xie, M.P Wang*, W. Chen, Y. Du

School of Materials Science and Engineering, Central South University, China

(Received 14 October 2017; accepted 29 June 2018)

Abstract

In the present work, texture evolution of AA7005 aluminum alloy during the accumulative roll bonding and conventionally rolled was investigated by X-ray diffraction. It was found that the dominant texture components of both samples were Brass, Copper, Rotated Cube and Goss components, but the ARB texture evolution was quicker and displayed complex features. When the number of ARB cycle increased, the intensity of texture components decreased at the second and third pass, then enhanced at the fourth pass, and finally decreased. During the ARB process there was a texture transition at the second and third pass from Brass and S to Rotated Cube components due to the shear texture which formed on the surface region and moved to the center during the next pass. The enhancement of texture intensity at the fourth pass might be attributed to the formation of nano shear bands. The texture intensity decreasing at final cycle was correlated to redundant shear strain and continuous recrystallization during the high ARB passes.

Keywords: *Accumulative roll bonding; Aluminum alloy; Conventional rolling; Texture evolution*

1. Introduction

Materials with ultra-fine grains (UFG, less than 1μm) show excellent mechanical properties such as high strength at ambient temperature, high corrosion resistance and high-strain-rate superplastic deformation at elevated temperature [1-5]. Severe plastic deformation has been found potential to produce such fine grain sized materials in bulk scale. By now, various SPD processes such as equal channel angular pressing (ECAP), high-pressure torsion (HPT) and accumulative roll bonding (ARB) have been proposed. Among these techniques, only ARB which was developed by Satio [1] is most appropriate for practical application because the process can be carried out by rolling mill without the use of a special die [6-8].

Although extensive studies have been conducted regarding the mechanical properties and microstructural evolution of materials processed by ARB [9-12], there is only limited quantitative information available about the texture evolution during this process. Texture analysis is a powerful tool to investigate the microstructural evolution during the deformation process. It has been shown that the texture evolution is different during the ARB process when compared to that of conventionally rolled samples [13]. The rolling textures of Al sheets are generally identified by an orientation fiber running through the orientation space from Copper orientation over S orientation to Brass orientation. Tsuji et al [14] pointed out that texture after ARB process is asymmetric and very weak in commercially pure Al. Kim et al. [15] also observed the presence of ideal Copper and Dillamore orientations at the center of the sample during ARB. They also pointed out that the texture of the ARB processed sheet has more complex features than that of conventionally rolled sheets. Chowdhury et al. [16] reported that the major texture components during ARB process can be characterized as the Dillamore component along with the S component with a scatter around the brass component in AA1100 alloy. However, the correlation between the texture evolution of the conventionally rolled samples and the ARB processed samples was seldom investigated [17]. The present research program is aimed at addressing this issue.

In the present study, a 7005 aluminum alloy was employed for the present investigation of texture evolution during the ARB process. The effect of number of ARB cycles on the deformation textures was also studied. As a reference, a sample with similar dimension was conventional rolled. In order to facilitate comparison, the final strain level was kept at

**Corresponding author:wangmp@csu.edu.cn*

DOI:10.2298/JMMB171014018X

the same level after each process. By comparing the texture evolution between both samples, a correlation between two processes was attempted.

2. Experimental procedure

The composition of the 7005 alloy used for present work is presented in Table 1. The initial thickness of the sample was 4 mm. The sheet was degreased in acetone and its surface was brushed by a steel brush to remove the surface oxide film. Then two sheets were stacked and bound strongly by wires through holes to ensure a firm contact and to prevent strips from slipping against each other during the rolling process. These two stacked sheets were heated at 473K for 5min, rolled to 50% thickness reduction without any lubrication in a single pass and finally air cooled. Roll-bonded sheet was then cut into two halves and stacked with a treatment described above. In order to prevent the propagation of edge cracks which appeared after several cycles, sample edges were trimmed and smoothed down before each following cycle. This process was repeated up to six passes to impart a total equivalent strain of 4.8. For conventional rolling, the 4mm sheet was rolled to four different strain levels, i.e. ε=0.8, 1.6, 2.4 and 3.2, and each sheet was also heated at 473K for 5min.

Table 1. *Chemical composition (wt %) of the alloy used in the present work*

Al	Zn	Mg	Mn	Cr	Cu	Fe	Si	Zr	Ti
Bal	4.6	1.4	0.24	0.12	0.05	0.25	0.22	0.11	0.03

Bulk texture of the conventional rolled and ARB processed samples were measured using X-ray texture goniometer based on Schulz reflection geometry using Cu-Kα radiation at a surface which is within 0.1mm from the sample center (RD-TD plane). Three incomplete pole figures ({111}, {200} and {220} pole) were measured and orientation distribution functions (ODFs) were calculated by LaboTex software using Bunge series-expansion method. Arbitrarily Defined Cells (ADC) algorithm was used and no restriction of specimen symmetry was imposed while calculating the ODFs.

The microstructure observation for the samples after ARB process was performed by FEI Tecnai G2 F20 field-emission transmission electron microscopy (TEM) at 200kV. Thin foils for TEM were polished by twin-jet electropolishing in a 210ml CH_3OH+90ml HNO_3 solution at 253K and at a voltage of 20 V.

3. Results

ODFs of the ARB processed samples were calculated from the pole figures and presented in Fig 1. Fig 1a represents the ODF after the first pass. The

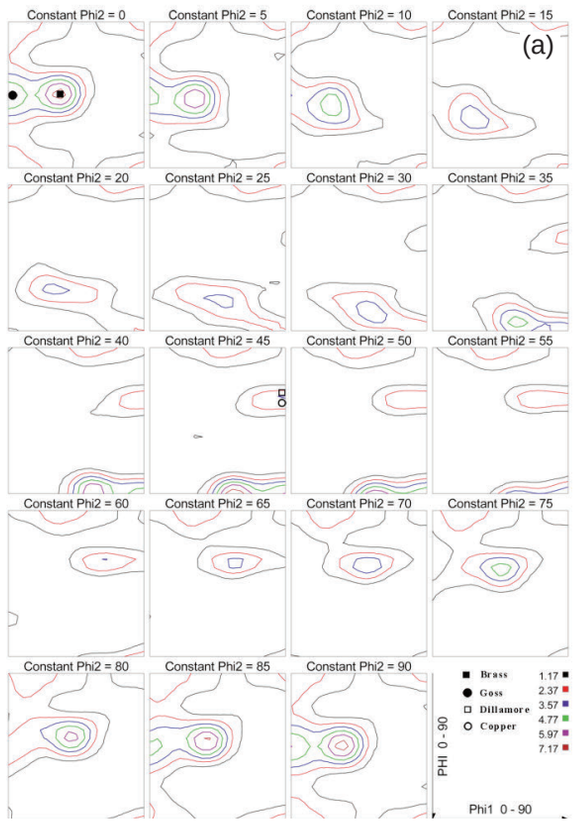

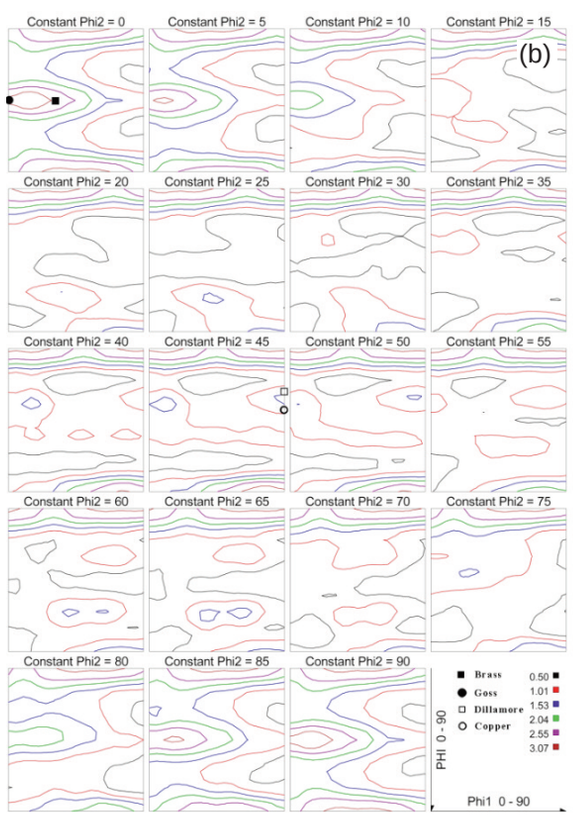

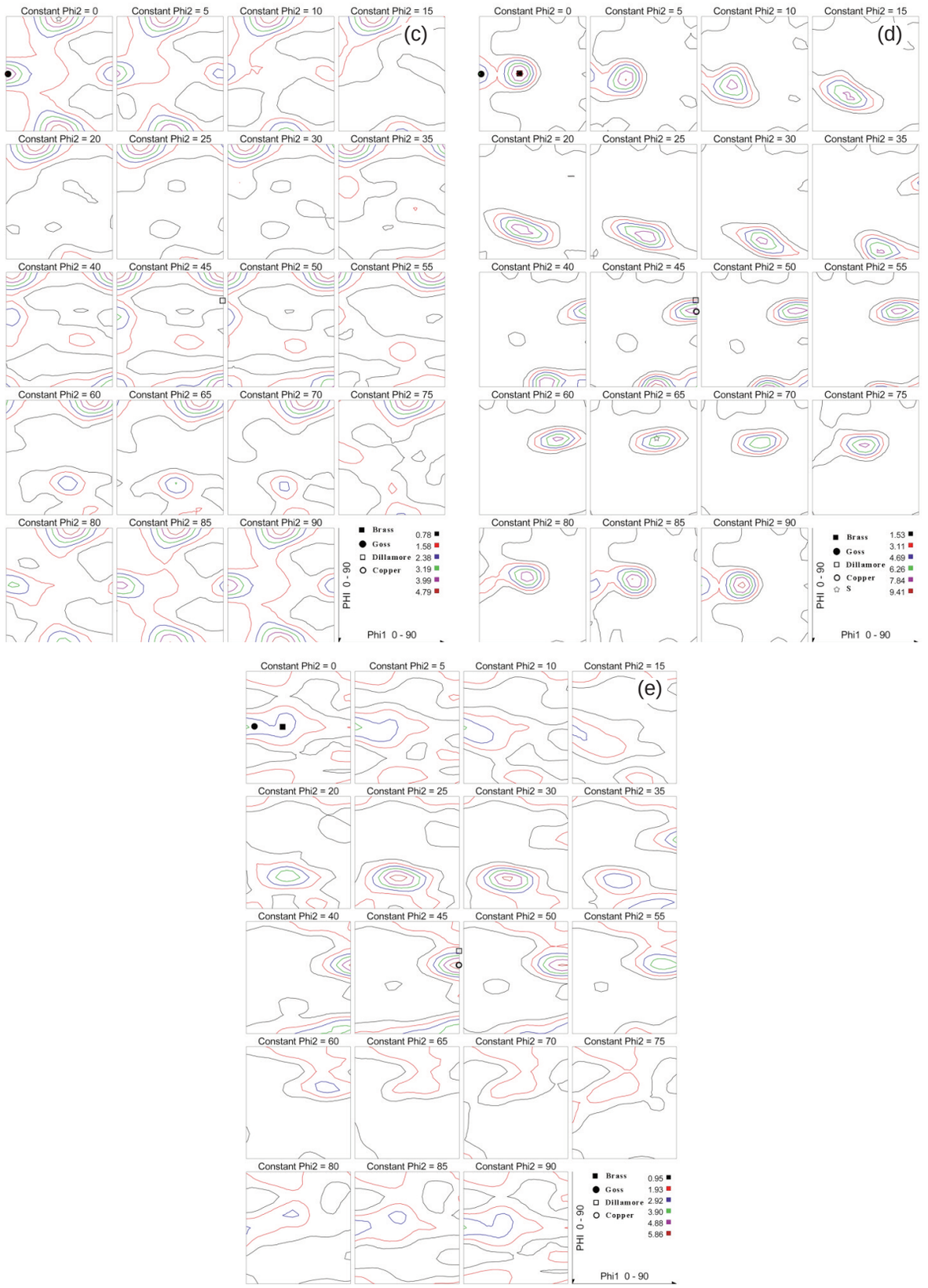

***Figure 1**.ODFs of ARB processed samples; (a) first pass; (b) second pass; (c) third pass; (d) fourth pass; (f) sixth pass*

textural components can be characterized as the brass component{0 1 1}<1 1 2>, Goss component { 1 1 0 } <0 0 1>, S component {1 2 3}<6 3 4> and copper component {1 1 2} <1 1 1> as well as the Dillamore component {4 4 11}<11 11 8>. After the second pass, as seen in Fig 1(b), the scatter around the components mentioned before reduced and the Rotated Cube appeared. After the third pass, a similar trend was observed. The brass component disappeared and changes appeared to the Goss and Rotated Cube components. However, after the fourth pass, clear brass, copper and Dillamore could be observed, and even the S component appeared. The most striking point here is that the overall texture intensity increased. After the sixth pass, the Copper and Dillamore components were more clearly visible and the intensity of the brass component got smeared a little.

The texture evolution can be demonstrated more thoroughly by the presentation of fibers during the course of rolling. Thus, the orientation density (f(g)) of main FCC fibers, including α,β and τ, was calculated from ODFs, as plotted in Fig.2. The α-fiber which shows from Goss {110} <110> to Rotated Goss{110}<110> components is presented in Fig.2a. Fig.2a shows that the texture evolution is centered mainly around the brass component for the first cycle. However, the brass component intensity decreases during the second and third pass. For the fourth pass, there is a remarkable promotion of the Brass and Goss components intensity. In the sixth pass, the Brass component intensity decreases.

Fig.2b represents the β-fiber running from the copper orientation {112} <111> over the S orientation {123} <634> to the Brass orientation {011} <211>. Generally, all samples show strong β-fiber textures with a preference for the Copper orientation. However, the β-fiber intensities of the fourth and sixth pass samples are stronger compared with other samples. As the ARB process continued further, first (after the second and third pass), the level of orientation intensities of the β-fiber decreases and then (after the fourth pass) increases.

The τ-fiber is presented in Fig.2c. After the first pass of the ARB process, the maximum intensity of the τ-fiber is located at Goss component and also there is another intensity peak at Φ=30°near Copper and Dillamore components. As the ARB process continue, during the second and third pass, another component which located at Φ=0° (Rotated Cube) increases. Referring to the α-fiber, it seems that there is a texture transition from Brass and Goss to Rotated Cube at the second and third pass. For the fourth pass, the Copper and Dillamore components are much stronger. The textural evolution of τ-fiber is centered mainly around Copper and Rotated Cube components. After the fourth pass, the Rotated Cube intensity decreases and the maximum intensity was located at Copper and Goss component. The sixth pass shape is similar to the fourth but the intensity slightly decreases.

The ODFs evaluated on samples after conventional rolling are presented in Fig.3. Fig.3

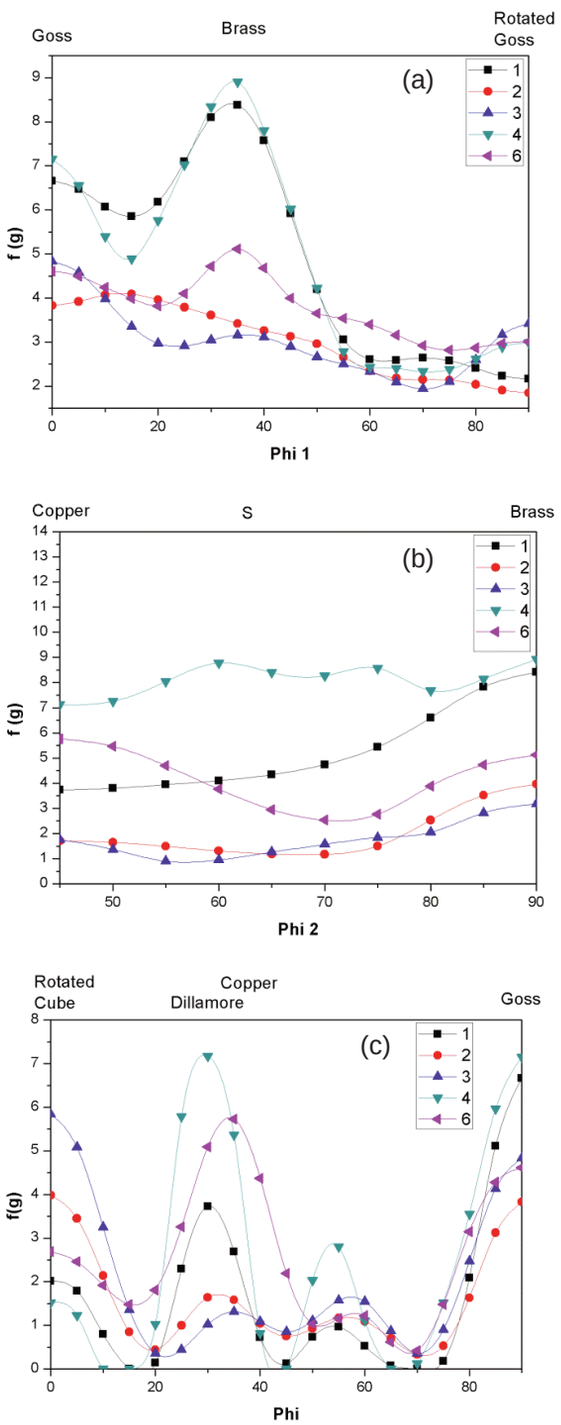

***Figure 2**. Fibers developed during ARB processing: (a) α-fiber, (b) β-fiber and (c) τ-fiber*

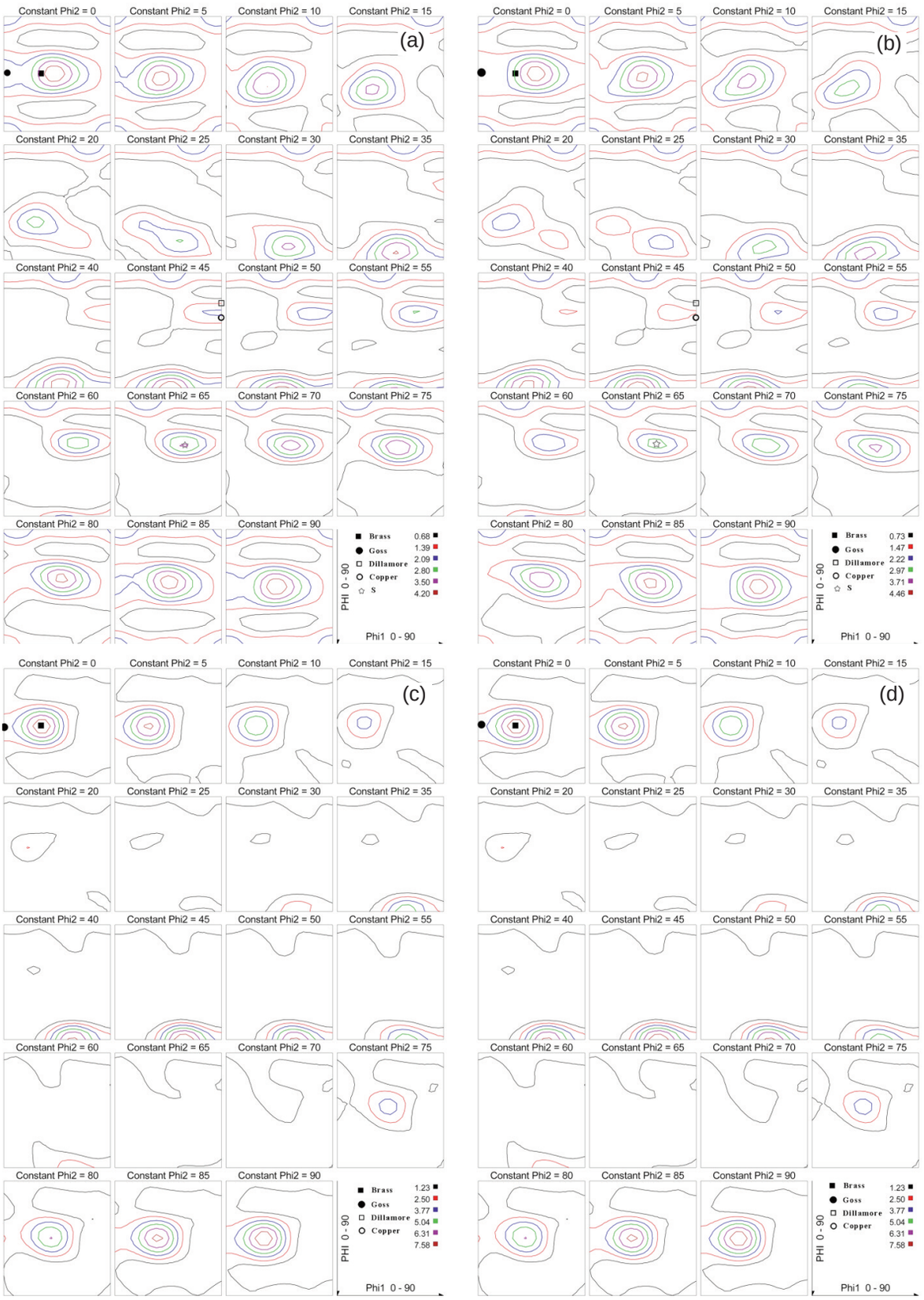

Figure 3. *ODFs of conventionally rolled samples: (a)ε=0.8; (b) ε=1.6; (c) ε=2.4; (d) ε=3.2*

shows the emergence of the normal texture components, i.e. brass component, Goss component and copper component. The difference in these figures is that the overall texture intensity of the samples enhances with the increase in the degree of rolling.

A comparison of the evolution of the fibers between the conventionally rolled sample and ARB processed samples is presented in Fig.4. The ARB

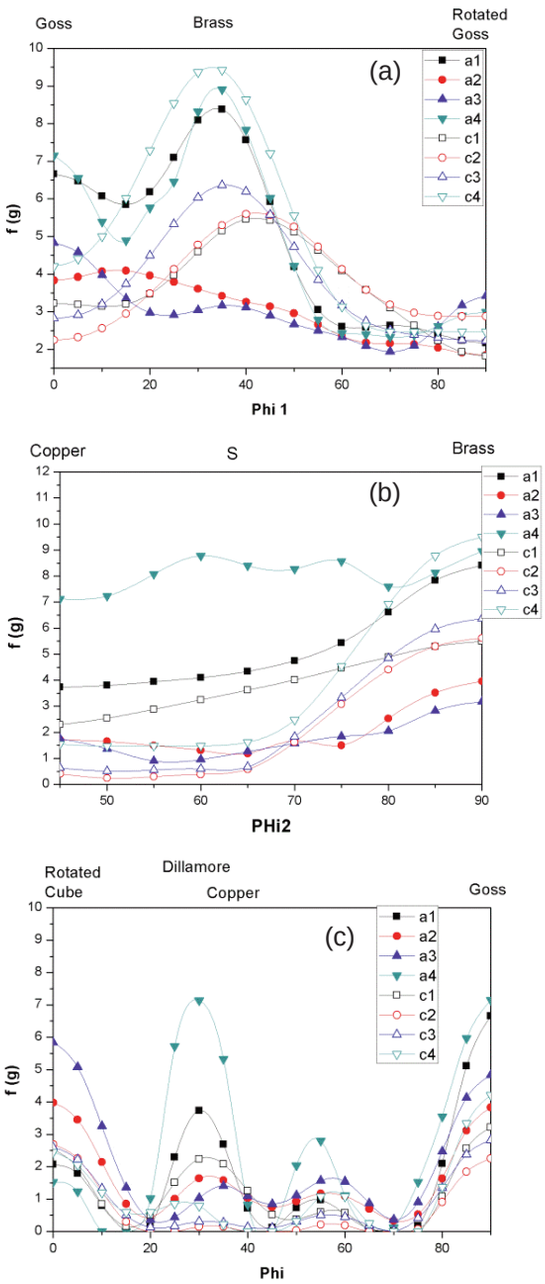

***Figure 4**. Comparison of evolution of fibers during conventional rolling and ARB processing at equivalent strain levels: (a) α-fiber, (b) β-fiber and (c) τ-fiber (a represents ARB sample, c represents conventional rolling sample)*

texture evolution shows more complex feature than conventionally rolled. Although in both cases the three major components brass, Goss and copper are present, the textural evolution between two samples is totally different at the same strain level.

With each pass, the texture component intensity of conventionally rolled sample simply increases. But the ARB sample is different. Fig.4a shows that the evolution of the brass texture component is being major in the α-fiber plot. In the conventional cold rolling samples, the brass component intensity simply enhances with the strain increase, however, this is different for the ARB process. The brass and Goss components decrease during the 2nd and 3rd pass and enhance during the 4th pass. The τ-fiber plot is presented in Fig.4c. For the conventionally rolled samples, they are nearly homogeneous, however, for the ARB samples, the Rotated Cube component of ARB increases during the second and third pass, and then it decreases during the fourth pass. The copper-type rolling texture by conventionally rolling can also be observed in the τ-fiber, but compared to the ARB sample, its intensity is weaker.

4. Discussion

In the present work, it is observed that, in both conventionally rolled and ARB processed samples, the major components are brass {011} <211>, Goss {110}<001> and Copper {112}<111> components, and the textural evolution between two kind samples is totally different at the same strain level.

Fig.4 shows that the ARB textural evolution is quicker and more complex than with the conventionally rolled samples. This result corresponds to the findings of Huang et al [18]. The texture component intensity increases with increasing cycles for conventionally rolled samples, but it shows more complex features for ARB samples. Compared to the conventionally rolled samples, each ARB cycle has a step to put the surface region into the center region during the next cycle so the shear texture will be destroyed and transformed into the rolling texture, but the conventionally rolling sample does not have this process. This is most important reason why ARB and conventionally rolled samples show different textural evolutions.

Another reason may be attributed to different microstructure evolution between conventionally rolled and ARB samples. Huang et al. [18] pointed out that the microstructural evolution in the ARB processed sample is much quicker than in the conventionally rolled sample. During the ARB process severe plastic deformation subdivides the initial grains into ultra-fine grain. In comparison to the conventionally rolled process, the ARB process means weak orienatation of the grain boundaries and

smaller spacing between lamellar boundaries. As mentioned before, ARB process has a step to put the surface region into the center region during the next cycle so the shear texture is drawn into the center region of the sheet, thus the ARB processed sample experiences a combination of rolling strain and shear strain. This may increase the local strain above the nominal strain corresponding to the thickness reduction.

As can be seen from ODFs and fiber plots, there is a texture transition at the second and third pass from Brass and S to Rotated Cube component. In the studies published by Mohammad [19,20], similar result is reported. There have been many attempts to explain the texture transition. The available literature suggests that the texture transition in FCC metals is primarily a result of the onset of planar slip and shear banding. Heason et al [6] reported that, duringthe ARB process without any lubrication, the surface region would form a single surface shear texture component, i.e. Rotated Cube{001}<110>. During the next pass, the surface shear texture was put into the center region, and this process is repeated. These results are in agreement with the present work. Heason [6] and Prangnell [9] all claimed that the strong texture developed during ARB, resulting from the weakening of Brass and S components in favor of strong Rotated Cube.

The intensity of texture components suddenly improved when the number of ARB pass increased up to fourth cycle. This result is consistent with the finding of other research. The TEM micrographs of the ARB sample at four passes and the conventional rolling sample at the same strain level are on Fig.5. In the 4-passes of ARB sample, sub-grains are surrounded by well-defined boundaries with a low dislocation density inside and the SAD pattern shows more complex shape than the pattern of the conventional rolling sample. Mohammad [20] all pointed out the reason for the remarkable increase of the component is attributed to the formation of nano shear bands in the microstructure, which is known to be associated with strong brass type texture. Nano shear bands are shear bands which size is less than 100nm. Mohammad [22] have observed the existence of nano shear bands by TEM and concluded that the formation of nano shear bands at the fourth ARB cycle facilities the development of Brass and Goss component. Hassan. S [23] explained that nano shear bands inclined between 20°and 45° towards RD and the Goss component nucleated at nano shear banding resulting in the brass component, so the formation of nano shear bands at the forth pass facilitates the development of the brass and Goss components.

As mentioned before, the Copper and Brass components intensity gradually increased in the fourth pass but decreased in the sixth pass. This can be attributed to the formation of equiaxed ultra-fine or even nano grains in the microstructure in the sixth pass (Fig.6). Fig.6 shows that the grain size was about 300nm or even less with ring-like SAD pattern became clear, indicating the increment of a fraction of high angle boundary. Many authors have analyzed the microstructure evolution during the ARB process [24]. For high ARB cycle, the microstructure changes to a layered structure separated by high angle boundaries. In the present work, the ARB process was carried out at 473K, and continuous recrystallization could easily have taken place in ultra-shear bands. The high angle grain boundaries subdivide the grains,

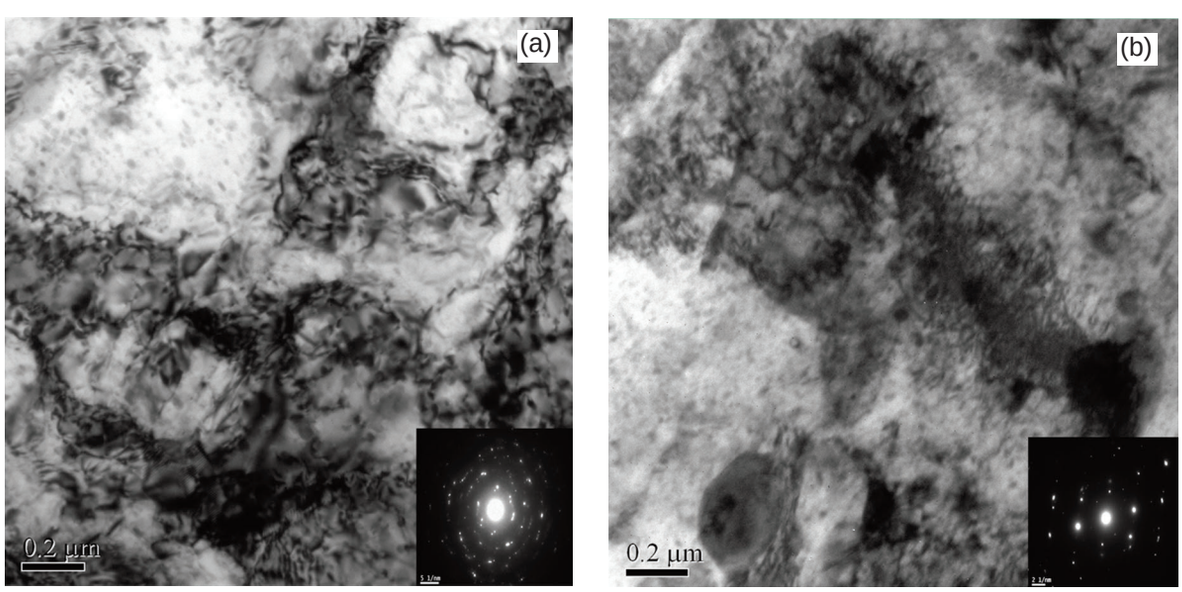

Figure 5. *TEM micrographs of ARB-processed sample after four passes and the conventional rolling sample at the same strain level (ε=3.2): a) ARB; b) conventional rolling*

meanwhile recrystallization occured in the ultra-shear bands thus the equixed ultra-grains form. Fig.5 revealed the formation of ultra-fine grain as a result of redundant shear strain and continuous recrystallization. Hence, the textural intensity decreased at sixth pass.

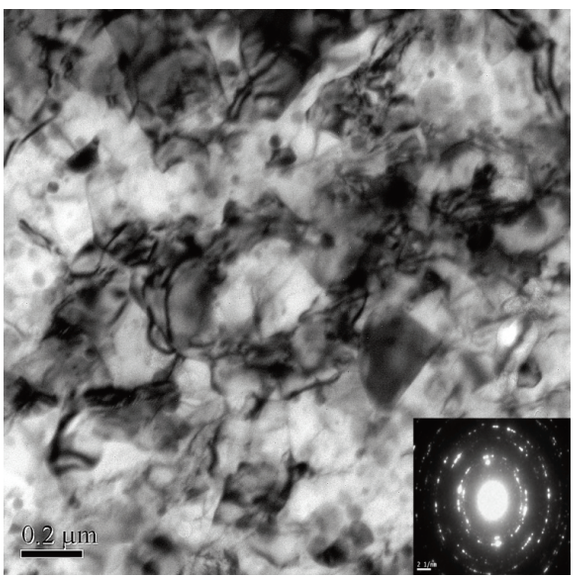

***Figure 6**. TEM micrograph of ARB-processed AA7005 after six passes*

5. Conclusion

In the present work, accumulative roll bonding was performed on AA7005 alloy up to sixth pass. The crystallographic texture evolution of the ARB-processed and conventionally rolled samples were investigated. Comparing the conventionally rolled samples to the ARB samples at the same strain, the ARB texture evolution was quicker and displayed more complex features. With each ARB cycle, the intensity of texture components decreased at the second and third pass, then it enhanced at the fourth cycle and finally decreased at sixth pass. The different textural evolution between conventionally rolled and ARB processed samples is attributed to special ARB rolling process which is needed to put the surface region into the center region during the next cycle and different microstructure evolution. As the ARB process continues there is a texture transition at the second and third pass from brass and S to Rotated Cube component because the shear texture which forms on the surface region should be put into the center during the next pass. The textural intensity enhancement during the fourth pass may be attributed to the formation of nano shear bands. Decrease of the texture intensity at final cycle was correlated to redundant shear strain and continuous recrystallization in the ultra-shear bands during high ARB cycles.

Acknowledgements

The authors are pleased to acknowledge the financial support by the National Natural Science Foundation of China (51271203) and the Nonferrous Metals Science Foundation of HNG-CSU (YSZN2013CL06).

References

[1] Y. Saito, H. Utsunomiya and N. Tsuji, Acta Mater., 47(2) (1999) 579-583.

[2] N. Kamikawa, N. Tsuji and N. Hansen, Acta Mater., 54(5) (2006) 55-66.

[3] P. B. Prangnel, J. R. Bowen and P. J. Apps, Mater Sci Eng A.,375A (2004) 178-185.

[4] N. Tsuji, Y. Saito and S.H. Lee, Advanced Engineering Materials., 5(5) (2003) 338-344.

[5] S. H. Lee and Y. Saito, Mater Sci Eng A., 325A (2002) 228-235.

[6] N. Hansen, X. Huang , N. Tsuji, Mater Sci Eng A., 387A (2004) 191-194.

[7] M. Karlik , P. Homola and M. Slamova , J. Alloys Comp., 378(1/2) (2004) 322-325.

[8] R. Z. Valiev, R. K. Islagaliev and I. V. Alexandrov, Prog Mater Sci., 45(2) 2000 103-114.

[9] H. Pirgazi , A. Akbarzaden and R. Petrov , Mater Sci Eng A., 492A 2008 110-117.

[10] R. T. Mohammad, A. Fakhreddin and H. Majid, Mater Sci Eng A., 556A (2012) 351-357.

[11] B. Azad, E. Borhani, J. Min. Metall. Sect. B-Metall. 52(1) B (2016) 93-98.

[12] J. S. Hayes, R. Kyte, P. B. Prangnell, Mater Sci Technol., 16(11/12) (2000) 1259-1263.

[13] S. R. Agnew, J. A. Horton and T. M. Lillo, Scripta Mater.,50(8) 2004 377-381.

[14] N. Tsuji , Y. Ito, Y. Satio, Scripta Mater., 47(12) (2002) 893-899.

[15] H. W. Kim, S.B. Kang, Z.P. Xing, Mater Sci Forum., 408/412 (2002) 727-732.

[16] G. S. Chowdhury, D. Abhijit and B. Ravikumar, Mater Sci Eng A., 428 A (2006) 351-357.

[17] B.N. Li, N.Tsuji and N. Kamikawa, Mater Sci Eng A., 423 A (2006) 331-342

[18] X. Huang, N. Tsuji N and N. Hansen, Mater Sci Eng A., 340 A (2003) 265-271.

[19] R. Mohammad, R.T. Mohammad RT and J. Roohollah, Mater Sci Eng A., 527A (2010) 68-73.

[20] M. Furukawa , Z. Horita , M. Nemoto, Mater Sci Eng A., 324 A (2002) 82-89.

[21] R. Mohammad, J. Roohollah and A. Jerzy, Mater Sci Eng A ., 527A (2010) 7068-7073.

[22] R.T. Mohammd, A. Fakhreddin and J. Roohollah, Mater Sci Eng A ., 556 A (2012) 351-357.

[23] S. Hassan , Scripta Mater., 64 (13) (2011) 556-559.

[24] W. Truszkowski, J. Krol J and B.Major, Metall Trans A., 11 (5) A (1980) 749-758.

UTICAJ AKUMULATIVNOG SPAJANJA VALJANJEM NA MENJANJE STRUKTURE I NJENO POREĐENJE SA LEGUROM ALUMINIJUMA AA7005 KOJA JE DOBIJENA UOBIČAJENIM VALJANJEM

H. Xie, M.P Wang*, W. Chen, Y. Du

Fakultet za nauku o materijalima i tehniku, Centralno-južni univerzitet, Čangša, Kina

Apstrakt

U ovom radu je ispitano menjanje teksture legure aluminijuma AA7005 tokom postupka akumulativnog spajanja valjanjem uz pomoć rendgenske difrakcije. Ustanovljeno je da su dominante komponente teksture u oba uzorka mesing, bakar, komponente u obliku zarotirane kocke, kao i Gos komponente, ali da je menjanje strukture tokom postupka akumulativnog spajanja valjanjem brže i da ta struktura ima složenije osobine. Kada se broj ponavljanja postupka akumulativnog spajanja valjanjem povećavao, intezitet strukturnih komponenti se smanjio tokom drugog i trećeg ponavljanja, a zatim se povećao tokom četvrtog ponavljanja, a zatim se opet smanjio. Tokom postupka akumulativnog spajanja valjanjem došlo je do promene strukture tokom drugog i trećeg ponavljanja, kada su mesing i S dobili oblik zarotirane kocke zbog deformacije koja je nastala smicanjem i koja se formirala na površini i zatim pomerila ka sredini tokom sledećeg ponavljanja. Intezitet strukture se tokom četvrtog ponavljanja poboljšao što se može objasniti formiranjem nano pojasa koji se formirao smicanjem. Intezitet strukture se smanjio tokom poslednjeg ponavljanja zbog prekomernog smicajnog opterećenja i neprekidne rekristalizacije tokom poslednjih ponavljanja postupka akumulativnog spajanja valjanjem.

Ključne reči: *Akumulativno spajanje valjanjem; Legura aluminijuma; Konvencionalno valjanje; Menjanje strukture.*